

VISCIOUS VORTICAL FLOW CALCULATIONS OVER DELTA WINGS

G. Blom, J. C. Wai, and H. Yoshihara
Boeing Military Airplane Company
Seattle, Washington

SUMMARY

Two approaches to calculate turbulent vortical flows over delta wing configurations are illustrated. The first is for a simple delta wing at low speeds using the boundary layer approximation to treat the effects of the secondary separation. The second is for the supersonic case of a generic fighter using the NASA Ames parabolized Navier/Stokes method. Test/theory comparisons are given in both cases.

INTRODUCTION

The concept of controlled separations due to D. Küchemann (ref. 1) plays an important role in the high lift performance of advanced combat aircraft. Here the sharp leading edges of the highly swept wing required for supersonic performance are parlayed into producing stable lift-generating leading-edge separation vortices. Such vortices can further serve as the base for a potentially powerful fast-response control system.

In the following, two cases of turbulent vortical flows are calculated. In the first, the low-speed flow over a slender flat plate delta wing at a large angle of attack is considered. Here the flow separates along the sharp leading edges forming the familiar primary separation vortices. Their effect, to a good approximation, can be treated by an inviscid theory. The primary vortices in turn impress an adverse pressure gradient on the upper surface boundary layer causing it to separate when the angle of attack is sufficiently large. The consequence of these secondary separations is to suppress significantly the suction peaks generated by the primary vortices. Our objective is the calculation of the displacement effects of the secondary separation, coupling the 3D integral boundary layer method with the leading-edge vortex panel method. The problem that must be resolved is the proper formulation (and solution) of the boundary layer problem and its convergent coupling with the inviscid problem.

In the second case, the supersonic flow over a generic fighter (Model -350) at large angles of attack is considered. Here a significantly more complex system of separation vortices arises which is shed from the wing and fuselage nose. For this complex flow the boundary layer approach used in the first case is no longer expedient. The flow is treated globally using the parabolized Navier/Stokes (PNS) equations with a mixing length turbulence model.

80555-084

THE BOUNDARY LAYER LIMIT LOW-SPEED DELTA WING*

The 3D integral boundary layer method used was developed by L. Wigton (ref. 3) and is essentially that of P. D. Smith (ref. 4). Here the planar Green's lag entrainment equations are embedded in the streamwise direction, and the transverse equations are derived assuming Mager's cross-flow velocity profile. The resulting system of equations is composed of four first-order partial differential equations containing six unknowns. It must be presumed that these equations become fully determinate when coupled to the equivalent inviscid flow problem. Since it is difficult to solve the problem in this global formulation, the solution is sought by an iterative procedure coupling the boundary layer and inviscid flows.

The resulting boundary layer problem is made determinate by assigning the values of two of the six unknowns. The choice of the two input functions must be such that the resulting boundary layer problem can be solved expeditiously for the separated case and that a convergent coupling with the inviscid flow can be achieved in a systematic fashion. We shall use the direct formulation of the boundary layer problem where the inviscid surface velocity components are used as inputs. By this choice there is a direct input/output compatibility between the boundary layer and inviscid flow problems. The resulting set of equations is fully hyperbolic permitting a finite-difference marching when the initial data lines are space-like. The limiting and inviscid surface streamlines form two of the four characteristics which define the domain of dependence.

For the problem of the secondary separation for the delta wing, we shall use the $x = \text{constant}$ lines (x is in the streamwise direction) which are proper initial data lines. The initial data to be assigned are not known in advance and must be determined by a "march/step back" procedure assuming the flow in the wing apex region to be conical. Once the initial data are established, a streamwise finite-difference marching is carried out using a first-order explicit differencing, biasing the lateral derivatives to cover the characteristic domain of dependence.

For severely separated cases ($\bar{H} \gtrsim 2.5$) an ill-conditioning of one of Green's equations arises caused by the derivative of the form factor function $\bar{H} = \bar{H}(\bar{R}_1)$ becoming very large (ref. 5). This ill-conditioning has been erroneously attributed to the appearance of separation with its envelope of limiting streamlines as well to the Goldstein singularity, but it is clearly due to the $\bar{H} = \bar{H}(\bar{R}_1)$ modeling required for the closure. The ill-conditioning can be circumvented by recalling that severely separated boundary layers assume an equilibrium state whereby the form factor \bar{H} is given directly in terms of the pressure gradient (ref. 6). The errant differential equation is then replaced by blending in the equilibrium flow as the ill-conditioning arises. Such large values of \bar{H} occur for example in the shock-induced and aft separations arising in the the transonic flow over swept wings, but they will not arise in the present case of the low-speed secondary separation.

(From Ref. 2)

For the low-speed case considered, the leading-edge vortex panel method is used for the equivalent inviscid flow. Here the leading-edge separation vortices are paneled as a potential vortex sheet, and their locations are determined by an iterative procedure. Since this panel method did not have provisions for viscous transpiration velocities, the upper surface viscous displacements were halved to approximate a wing camber change.

The first case considered was a flat plate delta wing of 76° sweep (aspect ratio = 1) at 11° angle of attack and a Reynolds number of 35×10^6 based on the 7.3 meter root chord. Boundary layer measurements were obtained by East (ref. 7). For this case, only the boundary layer was calculated inputting the measured surface velocity and flow direction. In figure 1 the calculated boundary layer variables are compared with the measurements, while in figure 2 the limiting streamline slopes are shown together with a comparison of the calculated and measured secondary separation lines. Good agreement is seen in both figures.

To illustrate the inviscid/viscid flow coupling, we have next considered the low-speed flow over the same flat plate delta wing at 20.5° angle of attack and at a smaller Reynolds number of 0.9×10^6 based on the 0.75-meter root chord. Wind tunnel tests were carried out for this case by Hummel (ref. 8). Four iterations between the panel method and the boundary layer solutions achieved a reasonable convergence. The resulting pressure distribution at two chordwise stations are shown in figure 3. Though the test/theory comparison is only fair, the theory appears to have yielded the general effects of the viscous displacement under the suction peak. The undesirable reexpansion near the leading edge is most probably due to the inadequate paneling of the free sheet adjacent to the leading edge. Here convergence of the vortex solution could not be achieved when a more refined paneling of the free sheet was used. The agreement of the pressures in the inboard region might be improved by incorporating the full transpiration velocity effects. With the relatively poor experience with the leading-edge vortex panel method, it would be desirable to repeat the calculations using the Euler equations with the proper viscous transpiration velocities.

In figure 4 the limiting streamline slopes are shown. Good test/theory agreement in the secondary separation line is found. Here also an oil-flow picture from reference 8 is shown. It should be noted that the Reynolds number was inadequate in the experiments to achieve natural turbulent flow. A radial boundary layer trip was required as shown in figure 4. The calculations were however carried out assuming the boundary layer to be fully turbulent.

PNS CALCULATIONS-SUPERSONIC MODEL - 350 FIGHTER

The calculations for the Model-350, shown in figure 5, were carried out under a NASA Ames/Boeing cooperative study. Other results from this effort were presented earlier by Dr. D. Chaussee (ref. 9). The Model-350 was selected since pressure distribution and boundary layer profile measurements were available (ref. 10).

The Ames PNS code was originally developed by L. Schiff and J. Steger (ref. 11). The PNS equations are the steady thin-layer Reynolds-averaged Navier/Stokes equations in which the pressure is assumed to be invariant across the subsonic portion of the boundary layer. The resulting equations can be marched in the streamwise direction when the inviscid flow is supersonic.

The bow shock from the fuselage nose is fitted, but all interior shocks arising farther downstream are captured as for example the Kutta shock from the trailing edge of the wing (fig. 6). A Kutta shock and an expansion fan are the dominant mechanisms by which the differing upper and lower surface flows adjust to form the wake. There is also a weaker "Kutta adjustment" through the subsonic sublayer embedding the trailing edge which is distorted by both the sublayer approximation in the boundary layer and the overlaying unphysically thickened shock (fig. 6). The consequence of this distortion is local and should not affect the overall lift.

The calculations were carried out for a Mach number of 2.2 and a Reynolds number of 4.3×10^6 based on the 2.4 foot mean wing chord. Angles of attack of 4° , 10° , 14° , and 18° were calculated, but only the results for 14° are presented. In figure 7 is shown the mesh at a wing station generated by an elliptic method. There are 45 points in the radial direction and 91 points along the half circumference. In figure 8 the calculated pressure distributions at 14° angle of attack are compared with the measured distributions at several streamwise stations. Good agreement is seen here consistent with the comparisons found at the other angles of attack. In figure 9 we compare the corresponding pitot pressure profiles in the boundary layer at several locations in a streamwise cut. The agreement in the profiles is reasonably good except where an inadequately refined mesh was used as at Station A. The inadequacy of the mesh here becomes evident by noting the steepness of the measured velocity gradient in the sublayer relative to the mesh used. The calculations have further yielded details of the profile as the "wobble" at the fuselage side (Station C) and on the wing (Station G) caused by a streamwise vortex which was detected from total pressure and vorticity maps. Thus to improve the overall test/theory match of the pitot profiles, one must refine the mesh in the sublayer, perhaps inserting a wall function to moderate the resulting computer cost.

In figure 10 the streamwise vorticity and Mach number contours in a transverse plane at a wing station are shown, while in figure 11 the corresponding transverse velocity vector map is given. Here the fuselage and wing vortices are evident. It is further seen that the separation on the wing originates not along the leading edge but at farther downstream points.

CONCLUDING REMARKS

Two levels of computing the viscous vortical flows over delta wing configurations at large angles of attack were demonstrated. In the first, the boundary layer method was used to determine the viscous displacement effects of the secondary separation over a flat plate delta wing at low speeds. Here the equivalent inviscid flow containing the primary separation vortices was

calculated using the leading-edge vortex panel method with the separation line fixed along the leading edge. The results indicated that the formulation of the boundary layer problem in the direct mode and the solution procedure were sound for the secondary separation but the leading-edge vortex panel method for the equivalent inviscid flow was inadequate. Here the substitution of the Euler code with provisions for viscous transpiration velocities would be desirable. The direct mode inviscid/viscid flow coupling did not offer any difficulties.

In the more complicated case of the Model-350 fighter a more global approach with the PNS method was used. Reasonable test/theory match was obtained for the surface pressure distributions and for the boundary layer pitot pressure profiles when an adequately refined mesh was used. Remarkably the algebraic Baldwin/Lomax turbulence model (basically the two-layer Cebeci/Smith model) continues to be a viable framework to treat complex viscous flows as the present one. There clearly is no immediate need to turn to more fundamental, though not necessarily more accurate, transport equation models that greatly increase the computer time.

The more widely recognized advantage of the PNS method relative to the ARC 3D method is the greatly reduced computing time due to the reduction of an unsteady problem to a steady one. A less obvious though a more important advantage for complex configurations as the Model -350 with nacelles and aft stabilizing surfaces is the resultant simplification of the mesh generation from a 3D to a 2D problem.

These significant advantages must be weighed against the shortcomings of the PNS method which preclude reversed flows and distort the elliptic influence mechanism through the thin subsonic portion of the boundary layer. The consequences of the latter however should not be of significance except where abrupt streamwise configuration slope changes arise, as at the leading edge of the wing root section or along the wing trailing edge, where large streamwise pressure gradients as shock waves are produced. Here the upstream influence through the subsonic portion of the boundary layer will be localized for turbulent flows in the absence of separation.

The experience with the two levels of treating viscous vortical flows suggests generally that the global approach with the Navier/Stokes method is the simpler more straightforward method for the user. Computer costs, particularly with the ARC 3D code, will continue to be a significant issue for some time. The boundary layer method will thus have its role of treating the simpler separated flows as those considered herein.

Finally we would like to express our gratitude to Dr. L. Schiff and Dr. D. Chaussee of NASA/Ames for indoctrinating us on the PNS code.

REFERENCES

1. Küchemann, D.: On the Possibility of Designing Wings that Combine Vortex Flows with Classical Aerofoil Flows. RAE T. M. Aero 1363, Oct. 1971.

2. Wai, J. C.; Baille, J. C.; and Yoshihara, H.: Calculation of Turbulent Separated Flow Over Wings. 3rd Symposium on Numerical and Physical Aspects of Aerodynamic Flows, California State Univ.-Long Beach, Cal., Jan. 1985.
3. Wigton, L.; and Yoshihara, H.: Viscous-Inviscid Interactions with a Three-Dimensional Inverse Boundary Layer Code. 2nd Symposium on Numerical and Physical Aspects of Aerodynamic Flows, California State Univ.-Long Beach, Cal. Jan. 1984.
4. Smith, P. D.: An Integral Prediction Method for Three-Dimensional Compressible Turbulent Boundary Layers. ARC R&M 3739, 1972.
5. Yoshihara, H.: Separated Flow Calculations in the B. L. Limit. Boeing TN BMAC 85-02, 1985.
6. East, L.; Smith, P. D.; and Merryman, P.: Prediction of the Development of Separated Turbulent Boundary Layers by the Lag Entrainment Method. RAE TR 77046, 1977.
7. East, L.: Measurements of the 3D Incompressible Turbulent Boundary Layer Induced on the Surface of a Slender Delta Wing by the Leading Edge Vortex. ARC R&M 3768, 1975.
8. Hummel, D.: On the Vortex Formation over a Slender Wing at Large Angles of Attack. AGARD CP-247, 1979.
9. Chaussee, D.; Blom, G.; and Wai, J. C.: Numerical Simulation of Viscous Supersonic Flow over a Generic Fighter Configuration. Sixth GAMM Conference on Numerical Methods in Fluid Dynamics, Gottingen, Sept. 1985.
10. Capone, F.J.; Bare, E. A.; Hollenback, D.; and Hutchison, R.: Subsonic/Supersonic Characteristics for a Tactical Supercruiser. AIAA Paper No. 84-2192, 1984.
11. Schiff, L.; and Steger, J.: Numerical Simulation of Steady Supersonic Viscous Flow. NASA TP 1749, 1981.

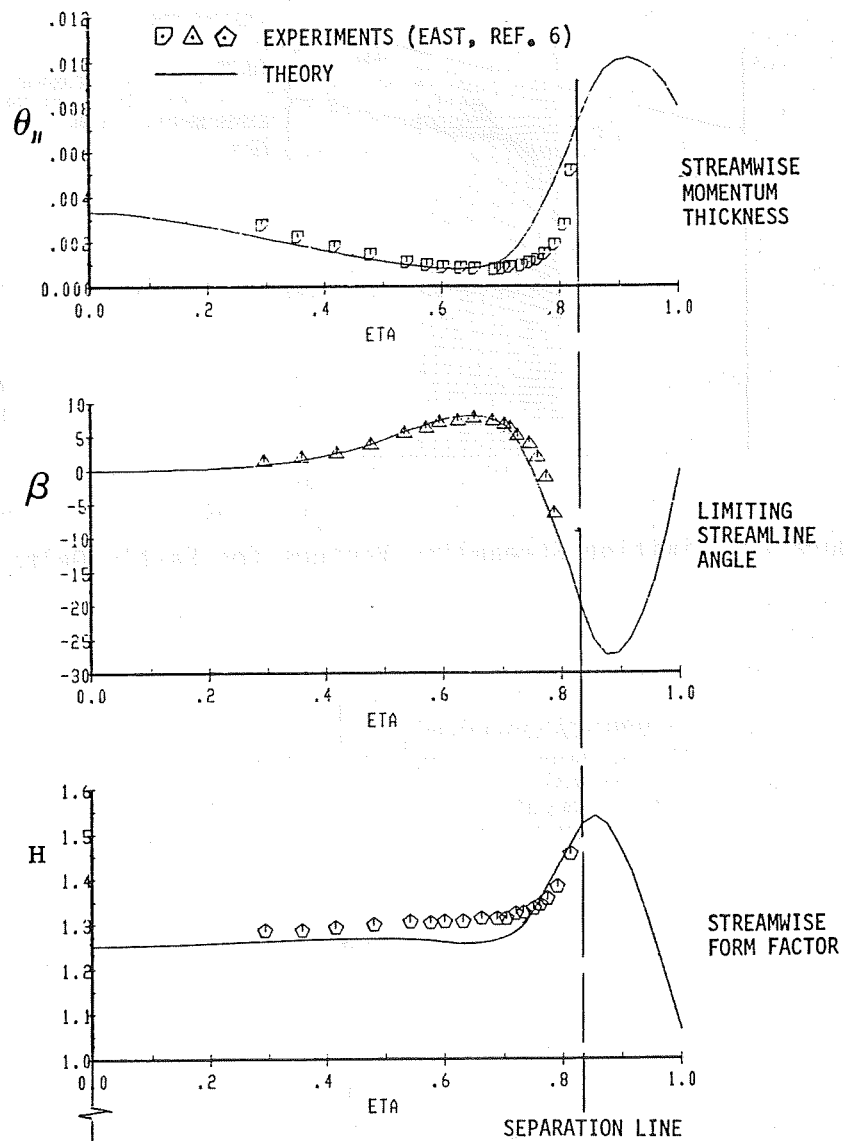


Figure 1. Test/Theory Comparison of Viscous Variables for East's Delta Wings

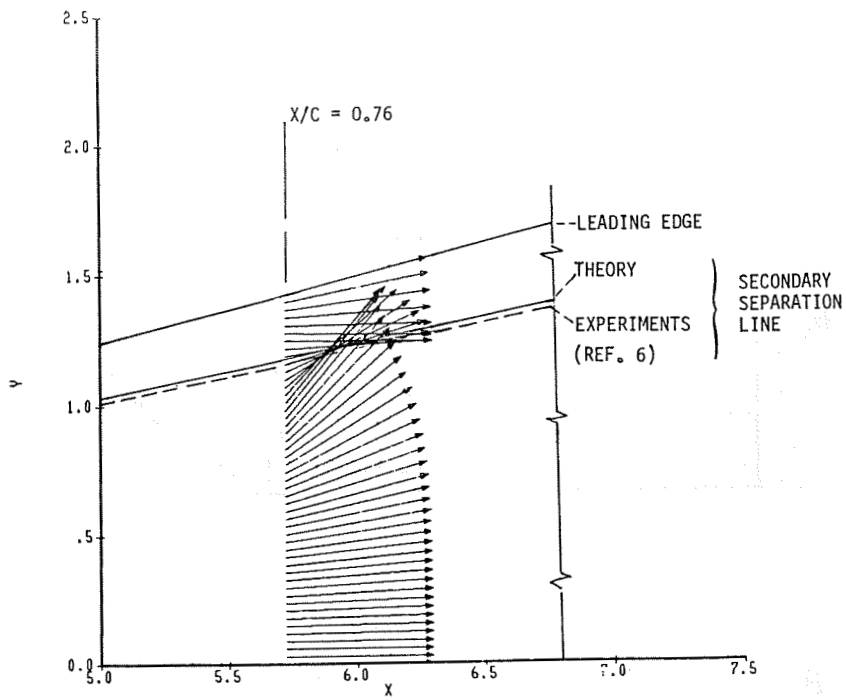


Figure 2. Limiting Streamline Vectors for East's Delta Wing.

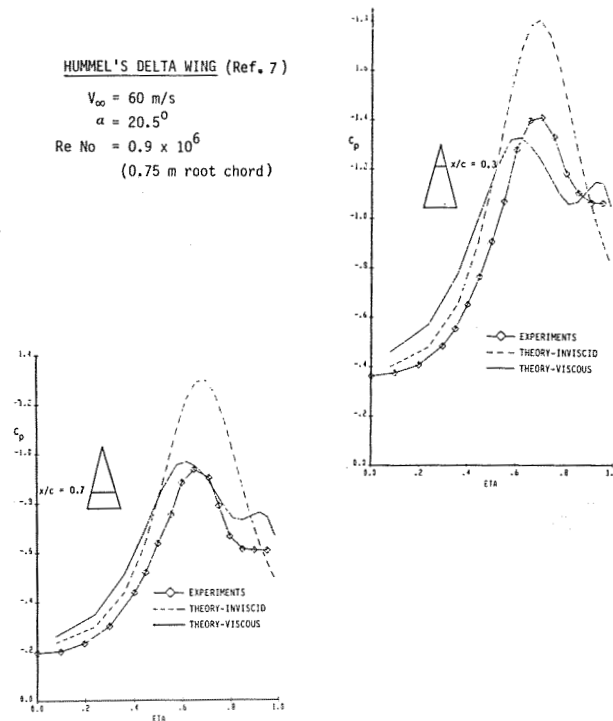


Figure 3. Test/Theory Comparison of Spanwise Pressure Distribution.

ORIGINAL PAGE IS
OF POOR QUALITY

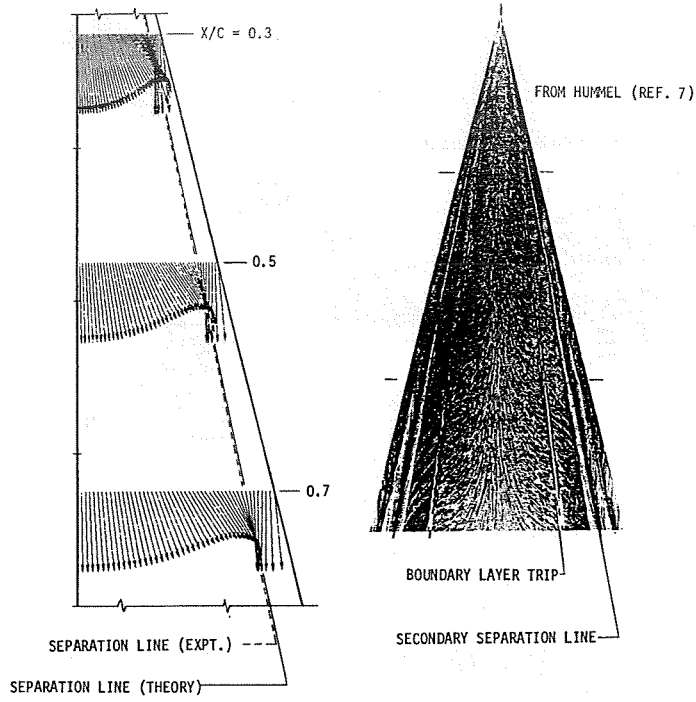


Figure 4. Limiting Streamlines and Separation Line of Hummel's Delta Wing.

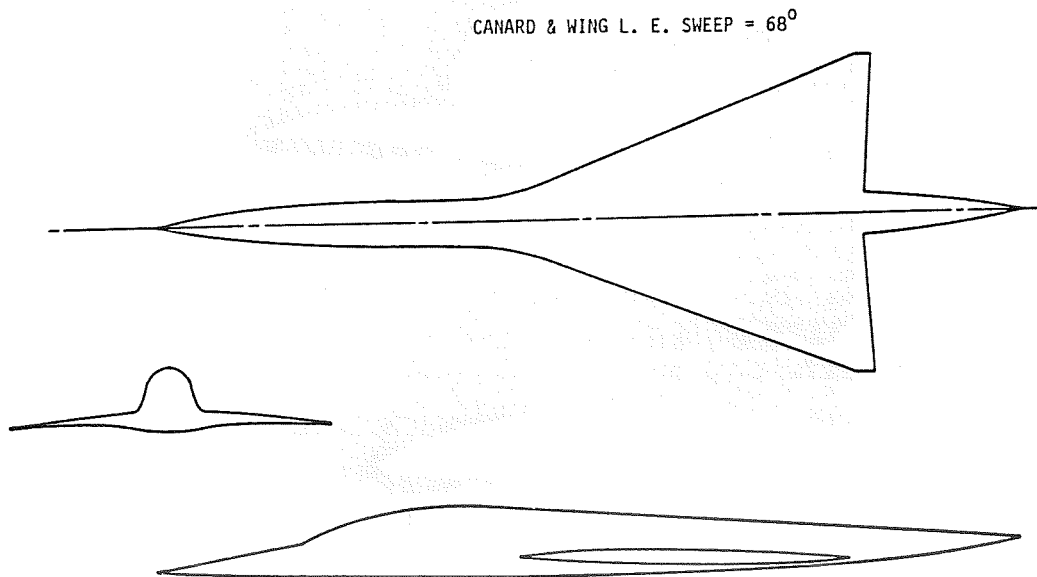


Figure 5. Model-350 Wing Fuselage.

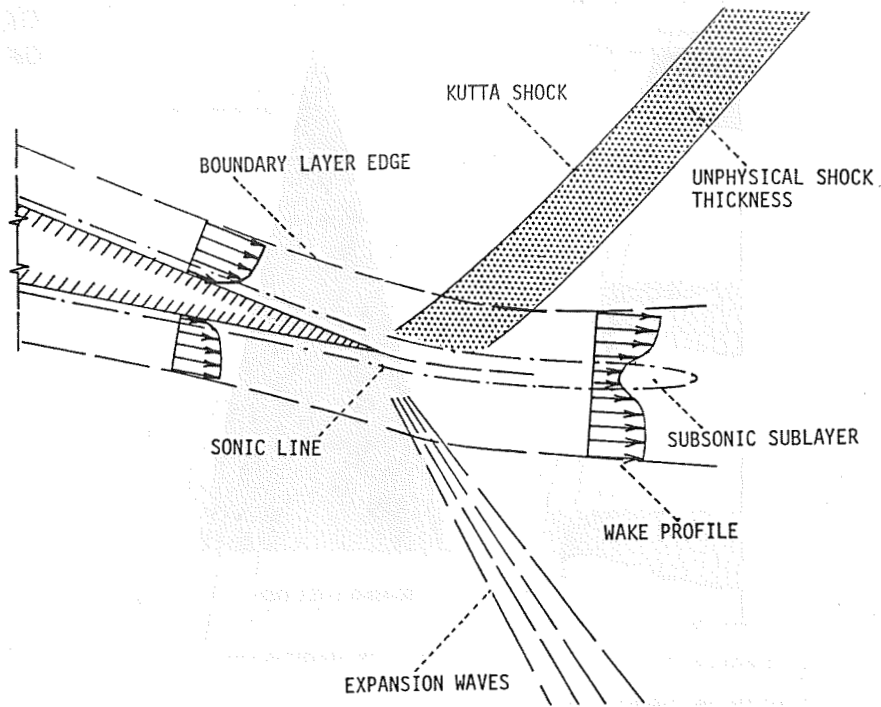


Figure 6. Schematic of Trailing-Edge Flow.

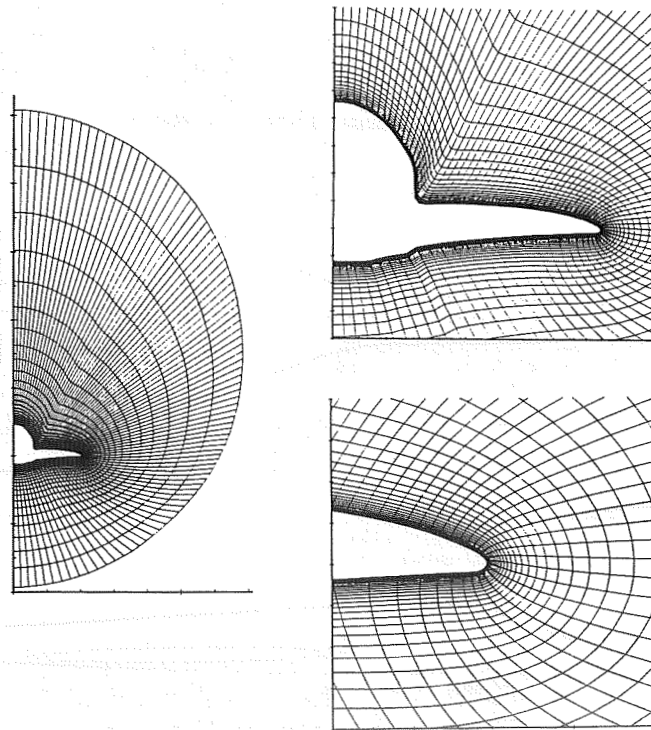


Figure 7. Elliptically Generated Wing Station Mesh.

ORIGINAL PAGE IS
OF POOR QUALITY

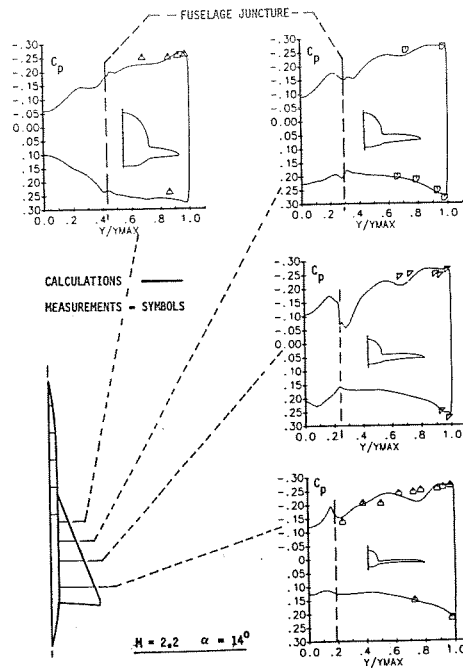


Figure 8. Test Theory Comparisons of Pressures.

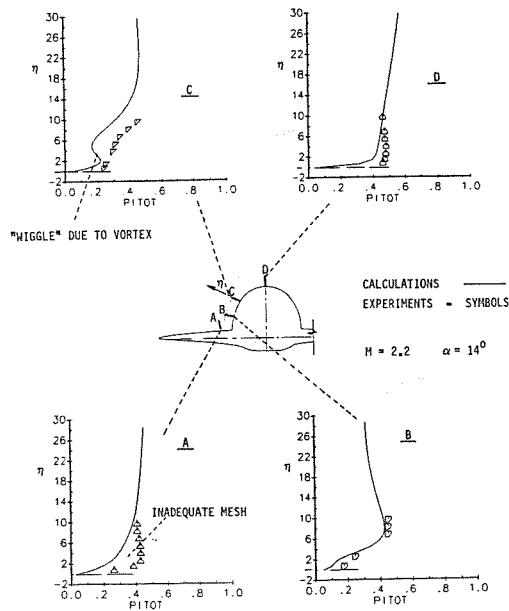


Figure 9. Test Theory Comparison of Pitot Pressure Profiles.

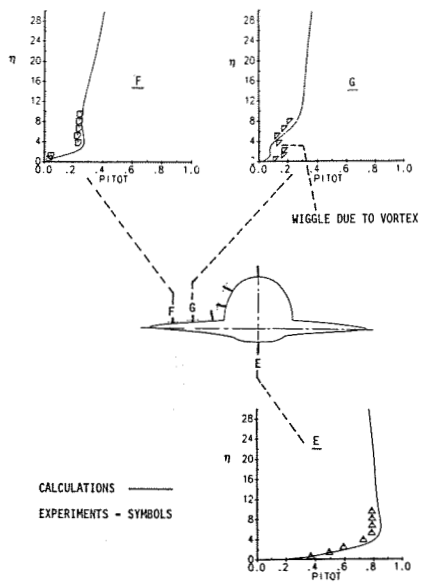


Figure 9. Concluded.

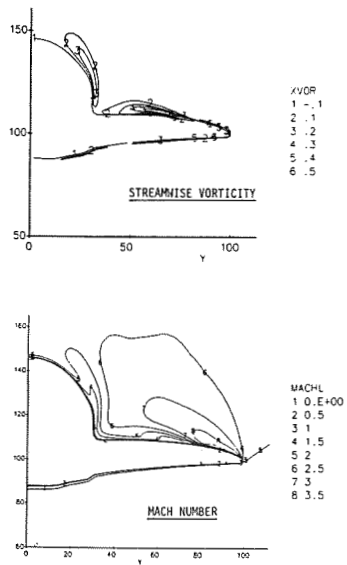


Figure 10. Streamwise Vorticity and Mach Number Contours.

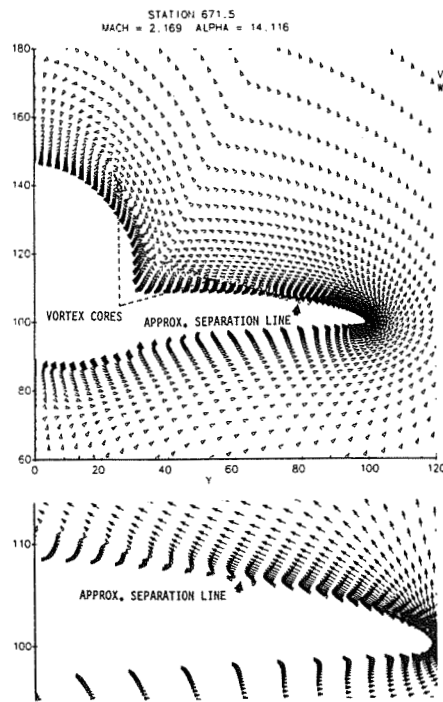


Figure 11. Transverse Velocity Vector Pattern.